



A flexible approach to combating chromatic dispersion in a centralized 5G network

M. A. Ilgaz*, K. Vuk Baliž, B. Batagelj

University of Ljubljana, Faculty of Electrical Engineering, Ljubljana, Slovenia
Trzaska Cesta 25, SI1000, Ljubljana

Article info

Article history:

Received 26 Nov. 2019

Received in revised form 01 Feb. 2020

Accepted 26 Feb. 2020

Keywords:

chromatic dispersion, opto-electronic oscillator, power penalty, radio access network, tunable dispersion-compensation module

Abstract

This article proposes and examines a solution in which the base-station for the fifth generation radio access network is simplified by using a single millimeter-wave oscillator in the central-station and distributing its millimeter-wave signal to the base-stations. The system is designed in such a way that the low-phase-noise signal generated by an opto-electronic oscillator is transmitted from the central-station to multiple base-stations via a passive optical network infrastructure. A novel flexible approach with a single-loop opto-electronic oscillator at the transmitting end and a tunable dispersion-compensation module at the receiving end(s) is proposed to distribute a power-penalty-free millimeter-wave signal in the radio access network. Power-penalty-free signal transmission from 10 MHz up to 45 GHz with an optical length of 20 km is achieved by a combination of a tunable dispersion-compensation module and an optical delay line. In addition, measurements with a fixed modulation frequency of 39 GHz and discretely incrementing optical fiber lengths from 0.625 km to 20 km are shown. Finally, a preliminary idea for an automatically controlled feedback-loop tuning system is proposed as a further research entry point.

1. Introduction

In today's sophisticated world, mobile communications are becoming increasingly important for human interactions, as well as human-to-machine and machine-to-machine connections. In the currently deployed fourth generation (4G) of wireless broadband communications for mobile devices, the so-called long-term evolution (LTE) standard, the radio access network (RAN), still suffers from certain drawbacks, such as a high latency and a limited bit rate. The latter being a consequence of the poor spectral efficiency and the limited bandwidth. The fifth generation (5G) RAN [1] aims to increase the bit rate and decrease the latency and power consumption [2-3]. In order to provide these improvements, millimeter-wave (mm-W) frequency bands are planned [4] for use in 5G RANs, in contrast to the microwaves used in current 4G RANs. A number of 5G

RAN field implementations have already started in many countries, but some challenges remain, such as providing lower latency and better synchronization [5-7].

In today's 4G RAN, the base-stations are already connected to the central-station via fiber-optic links. Such fiber connections are used for the distribution of a broadband information signal, as shown in Fig. 1. An optical fiber features low losses and high-bandwidth capabilities, compared to electrical or wireless links, and this means a low power consumption and data-rate increment. Nowadays, fiber-optic links are used for the distribution of telecommunications traffic to each base-station, where an opto-electronic conversion is made and an information signal up- and down-conversion is employed. Each base-station employs a local oscillator (LO) for the purposes of the up- and down-conversion of the signal from the photodetector or towards the laser diode [8]. It is expected in the future that optical technology or more specifically, technology of microwave photonics, will be integrated into 5G RAN architectures and bring advanced functionalities [9].

* Corresponding author: Mehmet Alp Ilgaz
e-mail: mehmet.ilgaz@fe.uni-lj.si

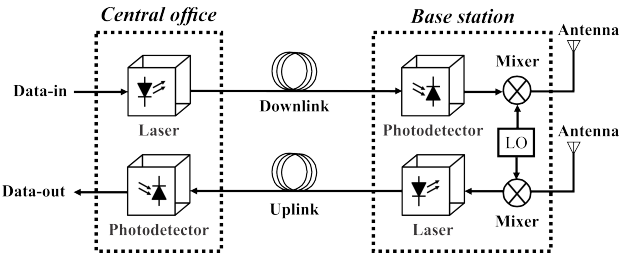


Fig. 1. Current configuration of a system working between a central-office and a base-station.

With the use of the mm-W band in next-generation 5G RANs, each base-station microwave oscillator needs to be replaced by a mm-W range oscillator. The stability requirements of such mm-W oscillators increase the complexity of the base-station, especially when a high spectral efficiency is demanded. Electronic oscillators in the mm-W range have a high phase noise since they use frequency multiplication, which provides a 6-dB phase-noise increase per octave. As such, complicated multi-doubling electrical techniques lead to a high-phase-noise mm-W signal, which results in a low spectral efficiency of the radio system. For this reason, in a 5G RAN the separation between the subcarriers is increased from 15 kHz to 120 kHz [10].

As opposed to the topology typical of a 4G RAN, it is expected that in a 5G RAN the phase noise will play a key role in achieving the quality of service. Since bit-rate requirements are constantly increasing, a higher-frequency bandwidth is required. This means that eventually the multiplex mm-W channels must be set further apart in order to avoid any interference from an adjacent channel. The undesirable phase noise of an electronic-oscillator signal worsens the situation by increasing the bandwidth even more. This problem can, however, be overcome by implementing an opto-electronic oscillator (OEO), generally offering a far lower phase noise (such as -163 dB/Hz at 6 kHz from a carrier [11]) than its electronic alternative. Furthermore, with the increasing bandwidth, higher carrier frequencies (in the mm-W region) are becoming of interest, which is yet another argument in favor of using an OEO. To the best of our knowledge, this is the first time a flexible solution for distributing an OEO-generated mm-W signal via a passive optical network (PON), while overcoming the issue of power fading, regardless of the frequency, by employing a tunable dispersion-compensation module (TDCM), has been proposed. This paper is an extended version of our previously presented idea at CSNDSP 2018. The preliminary idea for the implementation of a TDCM was presented and supported by simulation results in Ref. 12. In this paper we provide additional support for the preliminary idea with an extensive experimental work.

2. Single-loop opto-electronic oscillator

The single-loop OEO, the basic configuration of which is shown in Fig. 2, was invented in the mid-1990s, and today is one of the oscillators often used for radar and military applications because it can operate in the microwave and mm-W ranges. The OEO consists of a combination of

optical and electrical components and can provide electrical and optical outputs simultaneously. Thus, there is no additional opto-electronic conversion required when an output signal in the optical domain is needed. We will use this advantage in our novel network proposal.

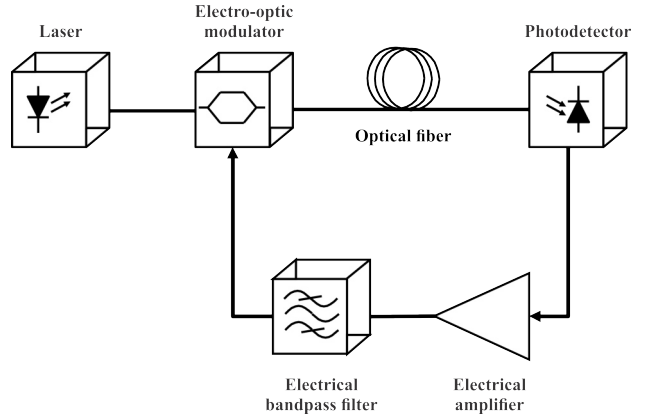


Fig. 2. Schematic of a single-loop OEO.

The OEO is composed of a laser, an external modulator, an optical fiber and a photodiode forming a delay line, also, an electrical amplifier and an electrical bandpass filter to provide the feedback. It is the optical fiber delay line that provides a high quality factor (Q-Factor) to the OEO, which is proportional to the length of the optical fiber. This means that the longer the fiber, the smaller the oscillator phase noise [13]. The relationship between the Q-Factor and the fiber length is shown in Eq. (1) [14]:

$$Q = \pi f \frac{nL}{c}, \quad (1)$$

where L is the optical fiber length, c is the speed of light in a vacuum, f is the oscillator frequency, and n is the refractive index.

One of the main advantages of an OEO, compared to other kinds of oscillators, such as the quartz-crystal oscillator, is that the phase noise is independent of the operating mm-W frequency, thanks to the resonator's properties [15]. In other words, it has a constant phase-noise characteristic with an increasing operating frequency. The phase noise with respect to the frequency offset from the OEO oscillation frequency is defined by Eq. (2) [15]:

$$S_{RF}(\Delta f) = \frac{\delta}{\left(\frac{\delta}{2\tau}\right)^2 + (2\pi)^2(\tau\Delta f)^2}, \quad (2)$$

where τ is the total group delay of the OEO loop, Δf is the offset frequency from the oscillation frequency of the OEO, and δ is the noise-to-signal ratio [15]. As it is clear from Eq. (2), the phase noise of the OEO is independent of the operating frequency. The noise-to-signal ratio of the OEO can be expressed as in Eq. (3) [15]:

$$\delta \equiv \frac{\rho_N G_A^2}{P_{osc}}, \quad (3)$$

where the noise density input ρ_N of the OEO is the sum of the thermal noise, the shot noise and the laser's relative intensity noise (RIN). An electrical bandpass filter is used

to select the operating frequency of the OEO from the multiple resonant peaks corresponding to the free spectral range (FSR) parameter. The electrical amplifier is used to compensate for the optical and electrical losses of the OEO loop. The response of the electrical bandpass filter is fixed; therefore, the OEO's output has limited tuning. In other words, the main oscillation mode's frequency range is limited by the electrical bandpass filter's bandwidth in the range of a few hundred MHz.

The OEO exists in many different configurations that target different performance goals, such as the greater suppression of side-modes, optimizing the phase noise, etc. The integrated OEO [16], dual-loop OEO [17], and injection-locked OEO [18], as well as the simple single-loop OEO are considered. The main parameters are compared in Table 1.

Table 1
Different configurations of the OEO.

Configuration	Integrated OEO [16]	Dual-loop OEO [17]	Injection-Locked OEO [18]	Single-Loop OEO [15]
Phase Noise (@10KHz)	<-50 dBc/Hz	-144.7 dBc/Hz	<-100 dBc/Hz	<-140 dBc/Hz
SMSR	N/A	145 dB	No visible side modes	N/A
Central Frequency	8.87 GHz	10 GHz	30 GHz	Up to 75 GHz
Delay Line Length	Several cm	1 km and 100 m	2.4 km	1 km

The configurations considered in Table 1 were invented for different purposes. The integrated OEO was designed to minimize the system size, whereas the dual-loop OEO and the injection-locked OEO were designed to improve the SMSR performance. In addition, optical solutions like photonic filters can be used instead of electrical bandpass filters for the frequency tuning of the OEO's output signal in the range of a few GHz or even more [19-22]. For instance, in Ref. 19 a microwave-photonics transversal filter is proposed to replace the electrical bandpass filter in the OEO's feedback loop. With such a configuration the output signal is tunable in the range of 4.09 – 9.7 GHz. The frequency is tuned by adjusting the optical source wavelength. In addition, an optical amplifier can replace the electrical one. Since the main goal of 5G RAN is to provide a low-phase-noise signal, we proposed a single-loop OEO with electrical components to provide a simple and easily configurable solution.

3. Discussion about the implementation of an OEO in a 5G RAN

The synchronization of the base-stations in a telecommunications network in previous technologies, such as 4G and earlier, is a critical parameter for data integrity, errorless data transmission and the hitless handover of subscriber connections between adjacent radio base-stations. The Global Navigation Satellite System (GNSS) receivers or the Precision Time Protocol (IEEE 1588) are the most widely used solutions for the synchronization of

such networks. Future plans for low-latency and increasing-bit-rate networks have created the need for the delivery of accurate and stable phase synchronization.

In order to accommodate future network requirements, we are proposing a more advanced synchronization-delivery scheme. To avoid any interference between the femto-cell base-stations and to coordinate these base-stations when broadcasting multimedia traffic, we propose a synchronization based on the distribution of the OEO's signal from the central-office to all the base-stations, as schematically depicted in Fig. 3.

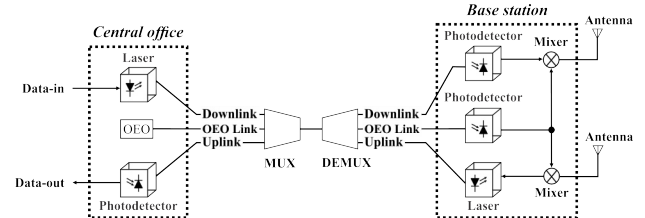


Fig. 3. Concept of an OEO implemented in a central-station and connected to a base-station with an analogue optical link.

The solution is based on our earlier synchronization solutions for the purpose of acceleration facilities, where phase stability in the sub-pico range was achieved [23]. Our approach is to employ the OEO in the central-office of each 5G RAN and distribute its low-phase-noise mm-W signal via a PON infrastructure. We propose to use a dark-fiber PON, since we will limit our scope to the wavelength of 1550 nm, although a separate wavelength can also be used in an existing PON system. The high-performance OEO can be placed in the central-office of the Cloud-RAN [24]. This brings the advantage that we can further simplify the base-stations of the current technology [25] and offer a solution that decreases the complexity problems of the 5G RAN. Since we remove all the LOs from the system and employ a single OEO in the central office, we believe that there will also be power savings in the 5G RAN. The centralized oscillator is easier to control because it can be placed in a closely controlled environment, compared to the solutions of current and previous technologies, i.e., 2G, 3G and 4G. Since all the base-stations have a common source of the oscillating signal that is distributed over the PON, the synchronization requirements of the 5G RAN can be more easily satisfied.

At this point there is already a lot of PON infrastructure interconnecting the central-station and the base-stations that is built of G.652D fibers [26]. Since such a fiber infrastructure is expensive to replace due to the necessary construction work, we expect to be dealing with issues related to chromatic dispersion, predominately the power penalty [27], which is typical of this type of fiber. The reason comes from different group velocities for the lower and upper sidebands in double-side-band modulation schemes, especially for the optical carrier wavelengths that are far from the zero-dispersion wavelength (1310 nm), e.g., 1550 nm. The power-penalty effect becomes substantial when the mm-W signal is transmitted through G.652D fibers.

The system shown in Fig. 3 is designed to use a 1550 nm laser as the optical source in the OEO. The main advantage of the 1550 nm wavelength, corresponding to the

3rd optical window, is the lowest point in optical losses (0.2 dB/km) in the entire optical domain. Thus, we chose to use the 1550 nm wavelength based OEO system for the 5G RAN. The DWDM can be used to transmit three links on the same optical fiber. The proposed system provides flexibility in sense that the operating oscillator frequency for the 5G RAN can be varied, as a TDCMs can be setup across the entire DWDM spectrum. One of the challenges of the 1550 nm wavelength OEO implementation for the mm-W range is the power penalty due to chromatic dispersion, which is dominant in the 1550 nm wavelength, especially for frequencies higher than 20 GHz [28]. The phase shift of each spectral component depends on the length of the optical fiber, the oscillator frequency and the dispersion coefficient. Consequently, for a given fiber the power of the detected signal is dependent on the optical length as, well as the frequency [29]. The power penalty in the electrical domain can be described with Eq. (4) [29]:

$$\text{Power penalty [dB]} = 10 \log \left(\frac{P}{P_0} \right) \propto 20 \log \left(\cos \left(\frac{\pi L D_{oc}}{c_0} (\lambda_{oc} f_{osc})^2 \right) \right) - 2\alpha L, \quad (4)$$

where P is the measured power of the system with an inserted fiber of the length L and P_0 is the measured power without a fiber (only a short patch cable connecting the modulator output and the photodiode), c_0 is the speed of light in a vacuum, D_{oc} is the fiber-dispersion coefficient, λ_{oc} is the optical carrier wavelength, f_{osc} is the oscillator frequency, and α is the fiber-loss coefficient (dB/km).

In order to explain the criticality of the power penalty, we demonstrate it in terms of the experimental work and the simulations. Figure 4 shows the experimentally measured and simulated results using Matlab for the power penalty as a function of frequency, considering a 1550 nm wavelength analogue optical link that is composed of a laser source with an external modulator, optical fiber and photodetector.

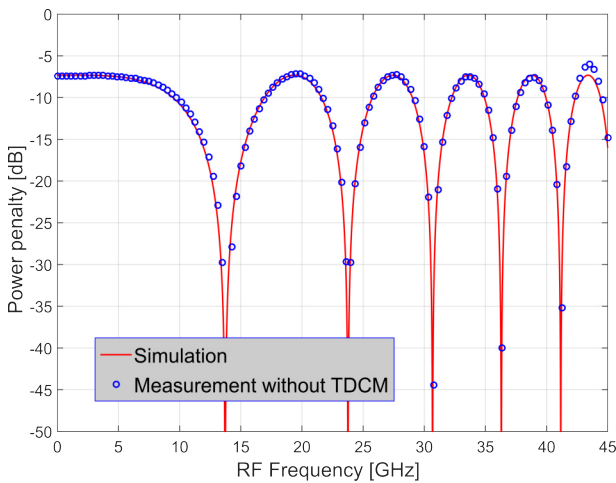


Fig. 4. Power-penalty measurement of a signal from 10 MHz to 45 GHz with an optical fiber length of 20 km.

The modulator is driven by an alternating voltage signal in the mm-W range, modulating an optical carrier, which represents the input signal of this analogue optical link, whereas its output signal is that on the electrical terminals

of the photodiode. It is obvious from the experimental and simulation results that chromatic dispersion is one of the phenomena affecting the optical signal's transmission through the G.652D fiber in the 1550 nm wavelength (the dispersion is of about 16.8 ps/nm/km). It is also obvious that the dispersion is more dominant in the mm-W range than in the microwave range.

4. The OEO system's implementation for a 5G RAN

Since we proposed using a single-loop OEO to meet the requirements of a 5G RAN, this section will explain the working principle in more detail. In order to provide the power-penalty-free mm-W signal distribution from the OEO, we employed a TDCM in each base-station, as shown in Fig. 5. Each TDCM is tuned individually according to the optical length of the PON branch in such a way that it ensures the constructive summing of both modulation side bands at the receiving end. Since the fiber spool in the OEO loop is not involved in the optical signal's transmission, we will only consider the power penalty introduced by the PON single-mode fibers.

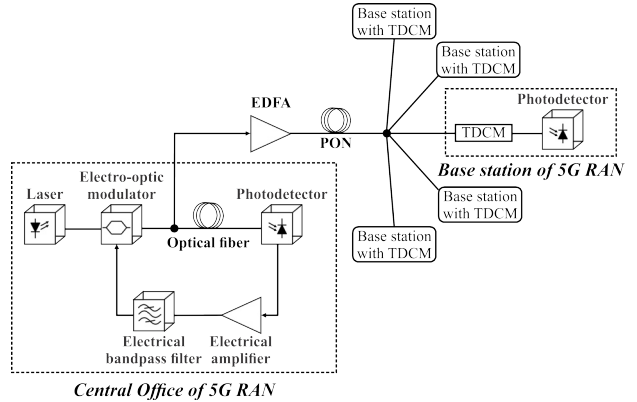


Fig. 5. OEO configuration for a 5G RAN in combination with a TDCM.

The EDFA is inserted between the PON and the OEO's optical output to compensate for the optical losses introduced by the PON. In order to maintain stability and not to increase the phase noise of the OEO, a low-noise electrical amplifier (based on a bipolar junction transistor) is selected for use at 39 GHz. The optical fiber of the OEO is as long as 1 km to optimize for the high Q-Factor, and thus to lower the phase noise.

Now we will describe the experimental setup to support the idea of avoiding the power penalty through the correct tuning of the TDCM for optical fiber different lengths. The test equipment consists of a vector network analyzer (VNA) that works up to 67 GHz, a 1549.32 nm distributed feedback (DFB) laser with an output power of 6.6 dBm, an external 40-GHz MZM with an insertion loss of 5 dB, and a V_π (half-wave voltage) of 4.3 V, an optical fiber path selector (having a connection with 0.625 km, 1.25 km, and 2.5 km fiber spools), a 5 km fiber spool, a 10 km fiber spool, a 20 km fiber spool, a TDCM, and a photodiode working up to 50 GHz. The TDCM operates at wavelengths between 1527.99 nm and 1567.13 nm and has an optical insertion loss between 3.3 and 4.1 dB. The TDCM used in the experimental setup is based on chirped fiber Bragg

gratings (FBGs) with thermoelectric coolers/heaters and can be tuned from -800 to +800 ps/nm. The experimental setup is the simplified configuration from Fig. 5. We do not insert an electrical amplifier and an electrical bandpass filter into the experimental setup since the required modulation signal is provided by the VNA. If we were to use the OEO instead of the VNA as a signal source in our experimental setup, like suggested by Fig. 5, we would only have been able to make the measurements for a single frequency. In that case only the length dependency of the chromatic dispersion effect, being a function of the fiber length, as well as the frequency, would have been experimentally evaluated. Nevertheless, our verification setup, shown in Fig. 6, allows us to perform the measurements with a reasonable frequency span of 45 GHz. A photograph of the experimental setup is shown in Fig. 7.

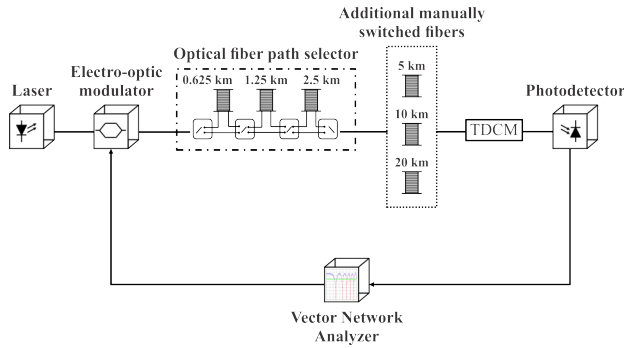


Fig. 6. Experimental setup of an OEO's configuration for a signal distribution from a central-station to a base-station.

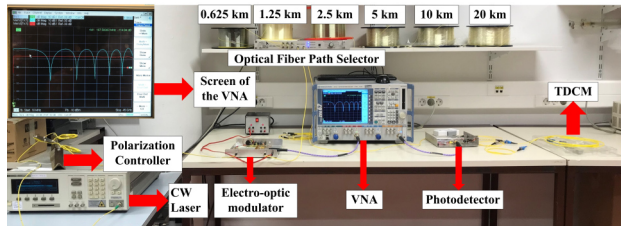


Fig. 7. Photograph of the experimental setup for avoiding chromatic dispersion by using a TDCM.

The experimental setup shows the OEO's signal distribution from the central-office to a single base-station. A single TDCM is placed in each base-station, which has a different optical length from the central-office according to the geographical position. Therefore, in each base-station the TDCM should be tuned individually based on its optical distance. According to the standard, the exact length of the PON branch should not exceed 20 km. Therefore, in the measurements we do not exceed an optical length of 20 km. The TDCM is set to compensate for dispersion according to the length of the optical fiber. For instance, if the length is of 10 km, the TDCM should be tuned to -168 ps/nm to achieve the optimal dispersion compensation.

In the first experiment we tuned the TDCM to a fixed value of -336 ps/nm to compensate for the dispersion of the 20 km PON and obtain the power-penalty-free transmission of the OEO signal. In the first measurement we do not need to use an optical fiber path selector because we only need one optical fiber length. We did the first measurement with

a 20 km fiber spool. The experimental results that correspond to the transmission with the TDCM are presented in Fig. 8.

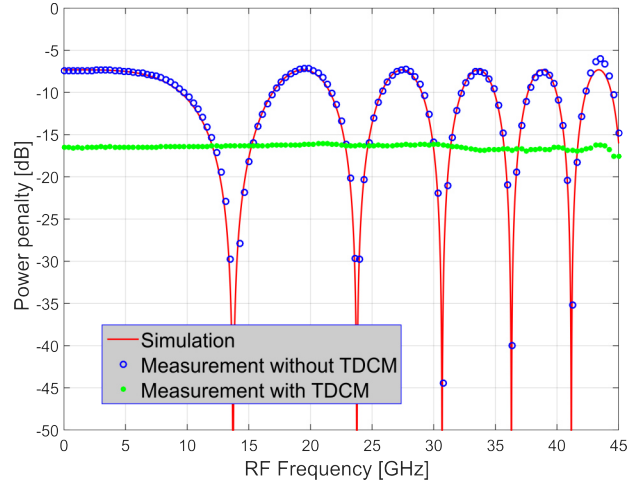


Fig. 8. Experimental results of the power-penalty measurement for a 20-km optical fiber with and without a TDCM. The operating frequency starts from 10 MHz up to 45 GHz.

As is clear from Fig. 8, a huge difference between the measurement of the power penalty with and without the TDCM is due to the precise compensation of a chromatic dispersion. The dispersion is compensated with respect to the TDCM; therefore, there is a dispersion-penalty-free transmission, but in a measurement without the TDCM optical signals are attenuated at various frequencies due to the power penalty.

In the next experimental case, we tune the TDCM from 0.625 km to 20 km with a step of 0.625 km to show that the power penalty is shifted due to the TDCM compensation. In order to achieve optical lengths of more than 4.375 km, we placed an additional 5 km and 10 km fiber spool as a series connection to the optical fiber path selector in the loop for the measurements between 5 km and 18.75 km. Plus, we have the result of the 20 km fiber from the first measurement. We selected 39 GHz as the source signal frequency as we believe that 39 GHz will be a useful frequency for the 5G RAN.

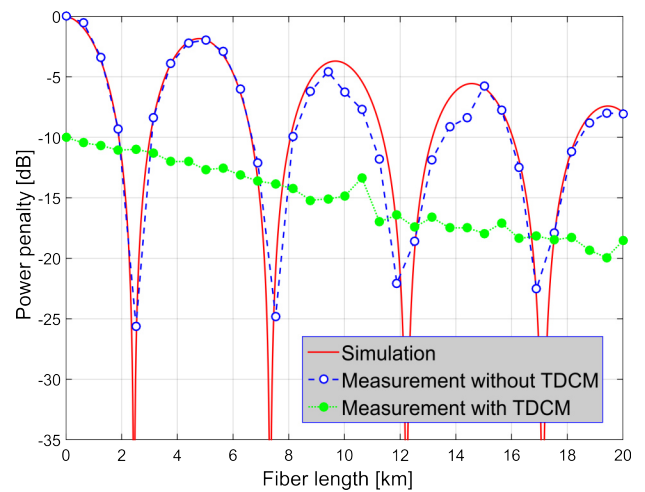


Fig. 9. Experimental results of the power-penalty measurement with an optical length from 0 to 20 km with an increment of 0.625 km.

As seen from the experimental results (Fig. 9), the TDCM is used to compensate for deep points, such as 2.5 km, 7.4 km, 12.3 km and 17.2 km in the optical fiber's length. The TDCM does add an extra insertion loss to the signal, but that can be compensated by adding an erbium-doped fiber amplifier (EDFA). Considering the experimental results based on the power-penalty measurements, we believe that our suggested configuration for the combination of a single-loop OEO and a TDCM would be useful for a 5G RAN. The main idea for the efficient OEO signal distribution to each base-station is in the accurate tuning of the individual TDCM towards the intelligent tunability in the base-stations.

Other than that, there are various approaches for distributing a mm-W frequency signal without a power penalty. Some of the offered solutions are summarized in Table 2.

Table 2
Different offered solutions to avoid a power penalty.

Property /Solution	DSF	DCF	FBG Filter	TDCM
Cost	(-)	(+)	(+)	(+)
Flexibility (RF)	(+)	(+)	(+)	(+)
Flexibility (optical wavelength throughout DWDM channels)	(-)	(-)	(-)	(+)
Flexibility (optical length)	(+)	(-)	(+)	(+)
Precision	(+)	(-)	(+)	(+)

One of the ways to solve the power penalty would be to replace the existing infrastructure build of a standard G.652D single-mode fiber with a dispersion-shifted fiber (DSF). While this solution is by far the most expensive one, it features wideband capabilities in the RF domain. It is, however, not flexible in terms of the optical wavelength, as any larger deviation from the zero-dispersion wavelength of the DSF in question results in chromatic dispersion effects.

The solution with a dispersion-compensated fiber (DCF) is in a similar price range as solutions 3 and 4. It offers wideband capability in the RF range, but it is not flexible in terms of the optical wavelength, as the dispersion coefficient is changing with the wavelength. Neither is it flexible in terms of the optical fiber length, as this changes the integral dispersion of the link.

A frequently suggested solution of FBG filters [30] for suppressing one of the sidebands in optical double sideband (DSB) modulation schemes is a cost-efficient solution, but it lacks flexibility in terms of changing the optical carrier wavelength.

The 1310 nm wavelength could be another possibility to avoid the power penalty since the chromatic dispersion is zero. The disadvantage of using the 1310 nm wavelength

is that optical losses are higher than for a 1550 nm wavelength, i.e., 0.2 dB/km at 1550 nm and 0.35 dB/km at 1310 nm. In addition, at 1310 nm, the optical nonlinearities are more dominant than at 1550 nm, since the chromatic dispersion is zero in the 1310 nm wavelength range [31-34]. Moreover, the EDFA does not operate at the 1310 nm wavelength and an EDFA is required for the implementation of the OEO's signal distribution from the central-office to the base-station via the PON to compensate for optical splitter's losses. The photonic-crystal fiber (PCF) [35,36] is another proposed solution to avoid the power penalty but replacing the PON with a PCF is very inconvenient in practice. All in all, we believe that our proposed solution with TDCMs in the base-stations outperforms other solutions with respect to all the parameters considered.

In Ref. 12 we already introduced an automatic feedback-loop tuning approach, which can be used for intelligent tuning. This operates in the electrical domain to enable the automatic adjusting of the TDCM compensating chromatic dispersion for each individual base-station. The idea of TDCM automatic control is depicted in Fig. 10.

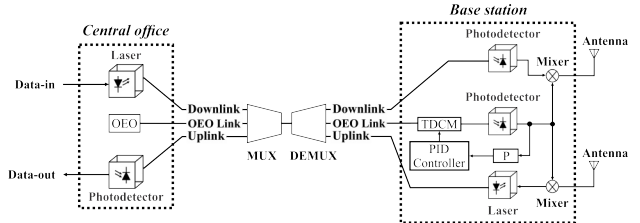


Fig. 10. Automatic control loop for a TDCM in each base-station to avoid the power penalty due to the chromatic dispersion.

As shown in Fig. 10, there is one option for automatic control of the TDCM. The electrical power meter is employed to measure the electrical power after the optical signal converted by the photodiode. Based on the measurement results from the power meter, the PID controller controls the TDCM to increase the signal power. When the maximum power is achieved, the tuning setting of the TDCM can be fixed.

5. Conclusions

In this article we have introduced the novel configuration of a single-loop OEO combined with a TDCM to distribute the mm-W signal to the base-stations in a 5G RAN. This is the first time that a TDCM has been employed to distribute a power-penalty-free mm-W signal with an arbitrary frequency. This proposed solution simplifies the base-stations by removing the LOs, providing a power-penalty-free mm-W signal and offering an improved synchronization approach between the central-station and the base-stations, while lowering electrical power consumption. Each base-station requires the TDCM to be tuned individually as the length from the central-station is different. Optimal tuning can be achieved with the proposed feedback-loop automatic control. With this, each base-station automatically tunes the TDCM and avoids any power penalty. With the TDCM and automatic control loop, all the base-stations will consist of the same components. Having the same equipment across all the

base-stations means lower equipment costs due to mass production and it also decreases installation, operating and maintenance expenses.

In this paper we showed experimentally how the chromatic dispersion invoking the power-penalty issue can be combated by the TDCM. The compensation was achieved for a wide-range frequency sweep and a fixed fiber length, as well as for a discretely varied (incremented) fiber length and a fixed mm-W frequency. We prefer to use the TDCM to avoid the power-penalty problem rather than other solutions. For instance, using a laser with a 1310 nm wavelength is another possible solution, but the signal with a 1310 nm wavelength has a higher optical loss and the optical non-linearities are more dominant in that region. Besides that, the OEO with a 1310 nm laser source will possibly have a higher phase noise due to the increased Rayleigh scattering. Other solutions such as an OEO combined with a DCF are neither universal nor flexible, since each base-station has a different optical distance from the central-station. This means that each base-station needs a DCF with different parameters and this only covers a single mm-W frequency or a narrow frequency range at best. Replacing the existing PON with a DSF or PCF is neither convenient nor cheap solution. Proposing a solution with a FBG is a low-cost solution, but it is not a flexible solution in the optical domain.

Based on the experimental work carried out we believe it would be possible to have a single mm-W OEO in the central-station as a flexible solution for a 5G RAN and distribute its signal to the base-stations of the 5G RAN without a power penalty.

Furthermore, the combination of the OEO with a TDCM could be used for various applications where a mm-W signal is required, such as radar applications, particle accelerators or radio-astronomy antenna arrays.

Beside the power-penalty problem of an OEO's implementation in a mm-W 5G RAN, there are other challenges. One critical challenge is the long-term stability of the OEO signal. This means that the OEO signal is shifted due to the temperature instability of some components in the oscillator loop (optical fiber, electrical filter). In other words, the OEO signal frequency is varying with time due to the ambient temperature swings. This can be solved with temperature stabilization of the optical fiber, an electrical bandpass filter, and a laser diode [37]. The need for temperature stabilization also supports our proposed idea of establishing the OEO at a single location (central-office), since it is easier to control and stabilize the ambient temperature of the central-office than the base-stations. Another challenge is the multi-mode operation [38] of the OEO, resulting in the so-called side modes in the oscillating signal. This problem can be solved by using optical solutions such as a finesse etalon [39] or a hybrid filter configuration [40] can be implemented to suppress the side modes instead of using electrical solutions.

Author statement

Research concept and design, M. A. Ilgaz and B. Batagelj; collection and/or assembly of data, M. A. Ilgaz and K. Vuk Baliž; data analysis and interpretation, M.A. Ilgaz, K. Vuk Baliž, and B. Batagelj; writing the article, M. A. Ilgaz, K. Vuk Baliž, and B. Batagelj; critical revision

of the article, M. A. Ilgaz, K. Vuk Baliž, B. Batagelj.; final approval of article, B. Batagelj.

Acknowledgements

The authors would like to express their gratitude to the company InLambda BDT d.o.o. for the research equipment and devices. The work presented in this article was carried out with the financial support of the Slovenian Research Agency (research core funding No. P2-0246) and the FiWiN5G Innovative Training Network, which has received funding from the European Union's Horizon 2020 Research and Innovation Program 2014–2018 under the Marie Skłodowska-Curie grant agreement No. 642355.

References

- [1] Sun, H., Zhang, Z., Hu, R. Q. & Qian, Y. Wearable communications in 5G: Challenges and enabling technologies. *IEEE Veh. Technol. Mag.* **13**, 3, 100-109 (2018). <https://doi.org/10.1109/MVT.2018.2810317>.
- [2] Andrews, J. G., Buzzi, S., Choi, W., Hanly, S. V., Lozano, A., Soong, A. C. K. & Zhang J. C. What will 5G be? *IEEE J. Sel. Areas Commun.* **32**, 6, 1065-1082 (2014). <https://doi.org/10.1109/JSAC.2014.2328098>.
- [3] Pirinen, P. A Brief overview of 5G research activities. in *1st International Conference on 5G for Ubiquitous Connectivity* (2014).
- [4] Patzold, M. It's time to go big with 5G [mobile radio], *IEEE Veh. Technol. Mag.* **13**, 4, 4-10 (2018). <https://doi.org/10.1109/MVT.2018.2869728>.
- [5] Andrus, B., Autenrieth, A., Pachnicke, S., Zou, S., Olmos, J. J. V., & Monroy, I. T. Performance evaluation of NETCONF-based low latency cross-connect for 5G C-RAN architectures. in *20th International Conference on Transparent Optical Networks (ICTON)* (2018).
- [6] Ren, H., Liu, N., Pan, C., Elkashlan, M., Nallanathan, A., You X. & Hanzo L. Low-latency C-RAN: An next-generation wireless approach. *IEEE Veh. Technol. Mag.* **13**, 2, 48-56 (2018). <https://doi.org/10.1109/MVT.2018.2811244>.
- [7] Lin, J.-C. Synchronization requirements for 5G: An overview of standards and specifications for cellular networks. *IEEE Veh. Technol. Mag.* **13**, 3, 91-99 (2018). <https://doi.org/10.1109/MVT.2018.2813339>.
- [8] Ilgaz, M.A. & Batagelj, B. Proposal for the distribution of a low-phase-noise oscillator signal in the forthcoming fifth-generation mobile network by radio-over-fibre technology. in *International Symposium ELMAR* (2016).
- [9] Capmany, J. & Muñoz, P. Integrated microwave photonics for radio access networks. *J. Lightw. Technol.* **32**, 16, 2849-2861 (2014). <https://doi.org/10.1109/JLT.2014.2333369>.
- [10] 3GPP Technical Specification Group Radio Access Network. NR, Physical layer procedures for control. TS 38.213 V15.3.0.
- [11] Eliyahu, D., Seidel, D. & Maleki, L. Phase noise of a high performance OEO and an ultra-low noise floor cross-correlation microwave photonic homodyne system. in *IEEE International Frequency Control Symposium* (2008).
- [12] Ilgaz, M.A. & Batagelj, B. Using tunable dispersion-compensated modules to overcome the power penalty of a millimeter-wave optoelectronic oscillator signal that is distributed via a passive optical network for 5G networks. in *11th International Symposium on Communication Systems, Networks & Digital Signal Processing (CSNDSP)* (2018).
- [13] Hao, T., Tang, J., Domenech, D., Li, W., Zhu, N., Capmany, J. & Li, M. Toward monolithic integration of OEOs: From systems to chips. *J. Lightw. Technol.* **36**, 19, 4565-4582 (2018). <https://doi.org/10.1109/JLT.2018.2825246>.
- [14] Hosseini, S. E., Karimi, A. & Jahanbakht, S. Q-factor of optical delay-line based cavities and oscillators. *Opt. Commun.* **407**, 349-354 (2018). <https://doi.org/10.1016/j.optcom.2017.09.077>.
- [15] Yao, X. S. & Maleki, L. Optoelectronic microwave oscillator. *J. Opt. Soc. Am. B* **13**, 8, 1725-1735 (1996). <https://doi.org/10.1364/JOSAB.13.001725>

- [16] Tang, J., Hao, T., Li, W., Domenech, D., Banos, R., Munoz, P., Zhu, N., Capmany, J. & Li, M. Integrated optoelectronic oscillator. *Opt. Express* **26**, 9, 12257-12265 (2018). <https://doi.org/10.1364/OE.26.012257>.
- [17] Lelièvre, O., Crozatier, V., Baili, G., Berger, P., Pillet, G., Dolfi, D., Morvan, L., Goldfarb, F., Bretenaker, F. & Llopis, O. Ultra-low phase noise 10 GHz dual loop optoelectronic oscillator. in *IEEE International Topical Meeting on Microwave Photonics (MWP)* (2016).
- [18] Lee, K., Kim, J. & Choi, W. Injection-locked hybrid optoelectronic oscillators for single-mode oscillation. *IEEE Photon. Technol. Lett.* **20**, 19, 1645-1647 (2008). <https://doi.org/10.1109/LPT.2008.2002743>.
- [19] Li, M., Li, W. & Yao, J. Tunable optoelectronic oscillator incorporating a high-Q spectrum-sliced photonic microwave transversal filter. *IEEE Photon. Technol. Lett.* **24**, 14, 1251-1253 (2012). <https://doi.org/10.1109/LPT.2012.2201462>.
- [20] Li, W. & Yao, J. An optically tunable optoelectronic oscillator. *J. Lightw. Technol.* **28**, 18, 2640-2645 (2010). <https://doi.org/10.1109/JLT.2010.2058792>
- [21] Li, W. & Yao, J. A wideband frequency tunable optoelectronic oscillator incorporating a tunable microwave photonic filter based on phase-modulation to intensity-modulation conversion using a phase-shifted fiber Bragg grating. *IEEE Trans. Microw. Theory Technol.* **60**, 6, 1735-1742 (2012). <https://doi.org/10.1109/TMTT.2012.2189231>.
- [22] Jiang, F., Wong, J. H., Lam, H. Q., Zhou, J., Aditya, S., Lim, P. H., Lee, K. E. K., Shum, P. P. & Zhang, X. An optically tunable wideband optoelectronic oscillator based on a bandpass microwave photonic filter. *Opt. Express* **21**, 14, 16381-16389 (2013). <https://doi.org/10.1364/OE.21.016381>.
- [23] Tratnik, J., Pavlovic, L., Batagelj, B., Lemut, P., Ritosa, P., Ferianis, M. & Vidmar, M. Fiber length compensated transmission of 2998.01 MHz RF signal with femtosecond precision. *Microw. and Opt. Tech. Lett.* **53**, 7, 1553-1555 (2011). <https://doi.org/10.1002/mop.26087>.
- [24] Checko, A., Christiansen, H. L., Yan, Y., Scolari, L., Kardaras, G., Berger, M.S. & Dittmann, L. Cloud RAN for mobile networks- a technology overview. *IEEE Commun. Surveys Tuts.* **17**, 1, 405-426 (2015). <https://doi.org/10.1109/COMST.2014.2355255>.
- [25] Ilgaz, M. A. & Batagelj, B. Preliminary idea for a converged fixed and mobile network infrastructure with 5G using radio-over-fiber technology and an opto-electronic oscillator in the millimeter-wave range. in *18th International Conference on Transparent Optical Networks (ICTON)* (2016).
- [26] Optical fibres, cables and systems. ITU-T Manual. 2009.
- [27] Patel, D., Singh, V. K. & Dalal, U. D. Assessment of fiber chromatic dispersion based on elimination of second-order harmonics in optical OFDM single sideband modulation using Mach Zehnder modulator. *Fiber Integrated Opt.* **35**, 4, 181-195 (2016). <https://doi.org/10.1080/01468030.2016.1195899>.
- [28] Gliese, U., Norskov, S. & Nielsen, T. N. Chromatic dispersion in fiber-optic microwave and millimeter-wave links. *IEEE Trans. Microw. Theory Technol.* **44**, 10, 1716-1724 (1996). <https://doi.org/10.1109/22.538964>.
- [29] Schmuck, H. Comparison of optical millimetre-wave system concepts with regard to chromatic dispersion. *Electron. Lett.* **31**, 21, 1848-1849 (1995).
- [30] Park, J., Sorin, W. V. & Lau, K. Y. Elimination of the fibre chromatic dispersion penalty on 1550 nm millimetre-wave optical transmission. *Electron. Lett.* **33**, 6, 512-513 (1997). <https://doi.org/10.1049/el:19970325>.
- [31] Matsuda, T., Naka, A. & Saito, S. Comparison between NRZ and RZ signal formats for in-line amplifier transmission in the zero-dispersion regime. *J. Lightw. Technol.* **16**, 3, 340-348 (1998). <https://doi.org/10.1109/50.661359>.
- [32] Naka, A. & Saito, S. In-line amplifier transmission distance determined by self-phase modulation and group-velocity dispersion. *J. Lightw. Technol.* **12**, 2, 280-287 (1994). <https://doi.org/10.1109/50.350593>.
- [33] Marcuse, D. Single-channel operation in very long nonlinear fibers with optical amplifiers at zero dispersion. *J. Lightw. Technol.* **9**, 3, 356-361 (1991). <https://doi.org/10.1109/50.70012>.
- [34] Lamminpää, A., Niemi, T., Ikonen, E., Marttila, P. & Ludvigsen, H. Effects of dispersion on nonlinearity measurement of optical fibers. *Opt. Fiber Technol.* **11**, 3, 278-285 (2005). <https://doi.org/10.1016/j.yofte.2004.11.002>
- [35] Wu, T.-L. & Chao, C.-H. A novel ultraflattened dispersion photonic crystal fiber. *IEEE Photon. Technol. Lett.* **17**, 1, 67-69 (2005). <https://doi.org/10.1109/LPT.2004.837475>.
- [36] Karim, F. Synthesis of dispersion-compensating triangular lattice index-guiding photonic crystal fibres using the directed tabu search method. *Opto-Electron. Rev.* **25**, 1, 41-45 (2017). <https://doi.org/10.1016/j.opelre.2017.04.006>.
- [37] Eliyahu, D., Sariri, K., Taylor, J. & Maleki L. Optoelectronic oscillator with improved phase noise and frequency stability. in *Proc. SPIE 4998, Photonic Integrated Systems* (2003).
- [38] Pan, S., Zhou, P., Tang, Z., Zhang, Y., Zhang, F. & Zhu, D. Optoelectronic Oscillator Based on Polarization Modulation. *Fiber Integrated Opt.* **34**, 4, 185-203 (2015). <https://doi.org/10.1080/01468030.2014.967895>.
- [39] Bagnell, M., Davila-Rodriguez, J. & Delfyett, P.J. Millimeter-wave generation in an optoelectronic oscillator using an ultrahigh finesse etalon as a photonic filter. *J. Lightw. Technol.* **32**, 6, 1063-1067 (2014). <https://doi.org/10.1109/JLT.2013.2294944>.
- [40] Liu, A., Liu, J., Dai, J., Dai, Y., Yin, F., Li, J., Zhou, Y., Zhang, T. & Xu, K. Spurious suppression in millimeter-wave OEO with a high-Q optoelectronic filter. *IEEE Photon. Technol. Lett.* **29**, 19, 1671-1674 (2017). <https://doi.org/10.1109/LPT.2017.2742662>.